Proc. Natl. Acad. Sci. USA
Vol. 96, pp. 11161–11166, September 1999
Biochemistry

Conversion of mammalian 3α-hydroxysteroid dehydrogenase to 20α-hydroxysteroid dehydrogenase using loop chimeras: Changing specificity from androgens to progestins

HAICHING MA AND TREVOR M. PENNING*

Department of Pharmacology, University of Pennsylvania School of Medicine, Philadelphia, PA 19104-6084

Communicated by Paul Talalay, Johns Hopkins University School of Medicine, Baltimore, MD, July 14, 1999 (received for review April 9, 1999)

ABSTRACT **Hydroxysteroid dehydrogenases (HSDs) regulate the occupancy and activation of steroid hormone receptors by converting potent steroid hormones into their cognate inactive metabolites. 3α-HSD catalyzes the inactivation of androgens in the prostate by converting 5α-dihydrotestosterone to 3α-androstanediol, where excess 5α-dihydrotestosterone is implicated in prostate disease. By contrast, 20α-HSD catalyzes the inactivation of progestins in the ovary and placenta by converting progesterone to 20α-hydroxyprogesterone, where progesterone is essential for maintaining pregnancy. Mammalian 3α-HSDs and 20α-HSDs belong to the aldo-keto reductase superfamily and share 67% amino acid sequence identity yet show positional and stereospecificity for the formation of secondary alcohols on opposite ends of steroid hormone substrates. The crystal structure of 3α-HSD indicates that the mature steroid binding pocket consists of 10 residues located on five loops, including loop A and the mobile loops B and C. 3α-HSD was converted to 20α-HSD by replacing these loops with those found in 20α-HSD. However, when pocket residues in 3α-HSD were mutated to those found in 20α-HSD altered specificity was not achieved. Replacement of loop A created a 17β-HSD activity that was absent in either 3α- or 20α-HSD. Once loops A and C were replaced, the chimera had both 3α- and 20α-HSD activity. When loops A, B, and C were substituted, 3α-HSD was converted to a stereospecific 20α-HSD with a resultant shift in k_{cat}/K_m for the desired reaction of 2×10^{11}. This study represents an example where sex hormone specificity can be changed at the enzyme level.**

Progress has been made in understanding the structural basis of steroid hormone recognition. Crystal structures of 3α-hydroxysteroid dehydrogenase (3α-HSD)·$NADP^+$·testosterone (1) and 17β-HSD·$NADP^+$·estradiol (2) ternary complexes have been elucidated. Also, atomic structures have been solved for domains of the progesterone and estrogen receptor occupied by their respective steroid ligands (3, 4). However, there are few examples where steroid hormone specificity has been altered by protein engineering. Success is most likely with structurally related proteins, and HSDs represent a reasonable starting point.

HSDs regulate the occupancy and activation of steroid receptors by converting potent steroid hormones into their cognate inactive metabolites (5). cDNA cloning indicates that virtually all mammalian 3α-HSDs and 20α-HSDs belong to the aldo-keto reductase (AKR) superfamily and are related (5–7). For example, rat liver 3α-HSD shows 67% amino acid sequence identity with rat ovarian 20α-HSD. In prostate 3α-HSD catalyzes the inactivation of androgens by converting 5α-dihydrotestosterone (5α-DHT) to 3α-androstanediol (8). Human type 2 and type 3 3α-HSD both are expressed in the prostate, catalyze this reaction, and share high sequence identity with rat liver 3α-HSD (9, 10). By contrast, 20α-HSD catalyzes the inactivation of progestins in the ovary and placenta by converting progesterone to 20α-hydroxyprogesterone (20α-OHP) (Fig. 1*a*). Progesterone is essential for maintaining pregnancy, and its metabolism to 20α-OHP is associated with the termination of luteal and placental stage pregnancy (11, 12).

The crystal structure of 3α-HSD·$NADP^+$·testosterone complex is characterized by the $(\alpha/\beta)_8$-barrel motif of AKRs. In this motif the α-helix and β-strand alternate eight times, and the β-strands coalesce in the core of the structure to form the staves of a barrel. At the top of the barrel loops exist (loops A, B, and C) that define the steroid hormone binding site (1) (Fig. 1*b*). Sequence similarity within this superfamily suggests that the 3α-HSD ternary complex is a good model for related HSDs.

Earlier studies showed that 3α-HSD displays no 20α-HSD activity (ref. 13, and J. M. Jez and T.M.P., unpublished data) and vice versa (14). Both enzymes catalyze 4-*pro*-R-hydride transfer from the C4 position of the nicotinamide ring to either the C3 or C20 ketone of their respective steroid hormone substrates (15, 16). Sequence alignments and predicted similarities of the three-dimensional structures of both enzymes show that the amino acid residues that bind NADP(H) are essentially invariant. Therefore NADP(H) is bound in the same orientation in both enzymes (6, 7), which implies that to convert 3α-HSD to 20α-HSD, the steroid binding pocket must be altered so that the steroid hormone substrate can bind in a backward orientation (D-ring at the A-ring position) and place the C17 side chain in proximity to the active-site residues.

In this study atomic models were used to predict which residues should be mutated to convert 3α-HSD to 20α-HSD. However, when all the substrate binding residues of 3α-HSD were mutated to the equivalent residues of 20α-HSD, this approach failed to yield the desired effect. Chimeric proteins then were generated by replacing the loops of 3α-HSD with the loops of 20α-HSD. The replacement of loop A created a bifunctional 3α/17β-HSD and importantly the 17β-HSD activity was absent in either 3α- or 20α-HSD. Once loops A and C were replaced, the resultant chimera was a bifunctional 3α/20α-HSD. When loops A, B, and C were changed, 3α-HSD successfully was converted to a stereospecific 20α-HSD with a resultant shift in k_{cat}/K_m for the desired reaction of 2×10^{11}.

MATERIALS AND METHODS

Materials. Primers used for PCR-based site-directed mutagenesis were synthesized by GIBCO/BRL. NAD(P)(H) were purchased from Boehringer Mannheim. All unradiolabeled steroids were obtained from Steraloids, Wilton, NH. [4-^{14}C] Progesterone (50 mCi/mmol) and [^{14}C] testosterone (50 mCi/mmol) were from NEN/DuPont. Restriction enzymes were purchased from

The publication costs of this article were defrayed in part by page charge payment. This article must therefore be hereby marked "*advertisement*" in accordance with 18 U.S.C. §1734 solely to indicate this fact.

PNAS is available online at www.pnas.org.

Abbreviations: HSD, hydroxysteroid dehydrogenase; AKR, aldo-keto reductase; 5α-DHT, 5α-dihydrotestosterone; 20α-OHP, 20α-hydroxyprogesterone.

*To whom reprint requests should be addressed at: Department of Pharmacology, University of Pennsylvania, School of Medicine, 3620 Hamilton Walk, Philadelphia, PA 19104-6084. E-mail: penning@pharm.med.upenn.edu.

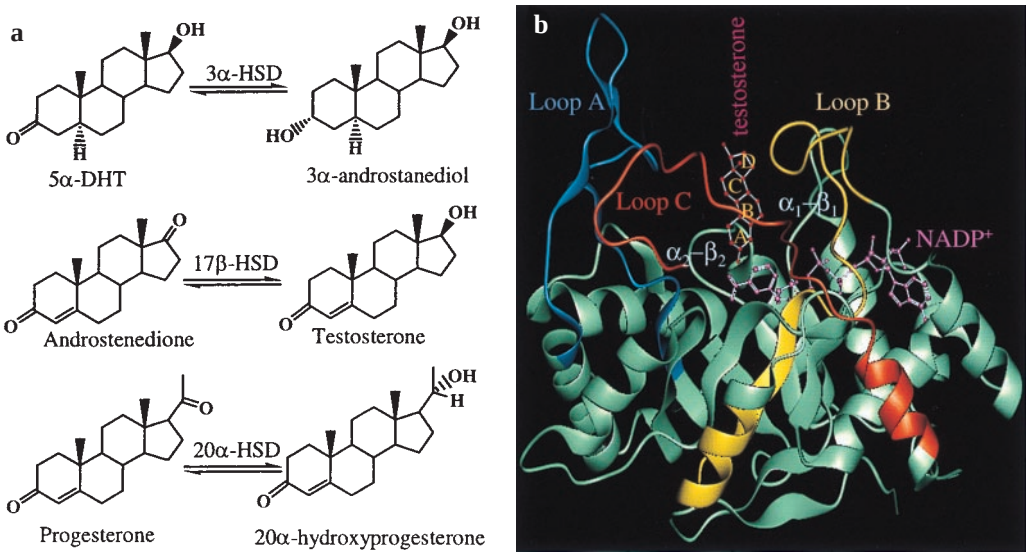

FIG. 1. (*a*) HSDs regulate the occupancy of steroid hormone receptors by converting potent steroid hormones into their cognate inactive metabolites. (*b*) The $(\alpha/\beta)_8$ barrel of 3α-HSD is turned on its side to show the positions of the five loops that comprise the mature steroid binding site. Testosterone is bound with its A-ring in the active site with its β-face toward the A-face of $NADP^+$. Colored fragments indicate the loops swapped in the chimeras. Loop A is blue, loop B is yellow, and loop C is red.

New England Biolabs, and other compounds were American Chemical Society grade and obtained from Sigma-Aldrich.

Site-Directed Mutagenesis of Substrate Binding Residues. Rat liver 3α-HSD cDNA was excised from the prokaryotic expression vector pKK3α-HSD (17) with *Nco*I and *Bam*HI and subcloned into the pET16b vector for optimal expression of mutants and chimeras. The prokaryotic expression vector pET-20α-HSD has been described (14). The following 3α-HSD mutants, F129L and T226Y/Y227C, were generated by two rounds of PCR, using the forward primers 5′-dTGGAGATATATTTTTACCAC-GAGATGAGC-3′ and 5′-dGGGAAGTTCACGAGACAAA-TACTGTGTGGATCAGAAAAGTCCAG-3′, respectively. The flanking forward and reverse primers were 5′-dCCG-GCTCGTATAATGTGTGGA-3′ and 5′-dCAGACCGCTTCT-GCGTTCT-3′, respectively. The N306F/Y310M mutant was generated by one round of PCR using the same flanking forward primer and the reverse primer 5′-dCGCCGCGGATCCCTAT-TCATCAGTAAATGGATGATTGGGATGGTCATCAAA-CATTTTTGCATTGAAGTATCTGAA-3′. The pKK-T24Y mutant was constructed by J. M. Jez and T.M.P. (unpublished data). The mutated nucleotides are underlined. The T226Y/W227C/N306F/Y310M was constructed by a single round of PCR using the T226Y/W227C mutant as template and the primers for the N306F/Y310M mutant. The F129L/T226Y/W227C and F129L/T226Y/W227C/N306F/Y310M mutants were constructed by ligating the *Nco*I fragment of the F129L mutant into the T226Y/W227C and T226Y/W227C/N306F/Y310M mutants, respectively. The T24Y/T226Y/W227C and T24Y/F129L/T226Y/W227C/N306F/Y310M mutants were constructed by ligating the *Hin*dIII fragment of the T226Y/W227C and F129L/T226Y/W227C/N306F/Y310M mutants into the T24Y mutant, respectively.

Generation of Loop Chimeras. The chimeras were generated by PCR amplification of the indicated loops, which then were swapped by using available restriction sites (Fig. 2). The Lp-A chimera (3α-HSD with 20α-HSD loop A) was generated in four steps. First, the N-terminal of 3α-HSD and the A loop of 20α-HSD were amplified separately by PCR using pET-3α-HSD and pET-20α-HSD as templates, respectively. The forward and reverse primers for amplification of the 3α-HSD N terminus were 5′-dCCGGCTCGTATAATGTGTGGA-3′ (a) (Fig. 2) and 5′-dATAGAGGTCCACATAGTCCA-3′ (b). The forward and reverse primers for the 20α-HSD loop A were 5′-dTGGACTAT-GTGGACCTCTAT-3′ (c) and 5′-dGCGGTTAAAGTTGGA-CACCCCG-3′ (d). These two PCR products were annealed and amplified by a second round of PCR using primers a and d to give a 3α-HSD N-terminal fragment containing loop A of 20α-HSD. This PCR product and the pET-3α-HSD vector were digested at the two *Nco*I sites; the desired fragment with loop A of 20α-HSD was ligated into the truncated pET-3α-HSD.

The Lp-B chimera also was generated in four steps. First, the C terminus of 3α-HSD and the loop B of 20α-HSD were PCR-amplified. The forward and reverse primers for the C terminus of 3α-HSD were 5′-dCCAGTTCTCCTGGAT-GATCC-3′ (e) and 5′-dCCCGGATCCAGGAGCTTCGAG-CAGAACAC-3′ (f). The forward and reverse primers for loop B of 20α-HSD were primer c and 5′-dGGATCATCCAG-GAGAACTGG-3′ (g), respectively. These PCR products were annealed and amplified by a second round of PCR with primers c and f to give a fragment containing the 3α-HSD C-terminal fragment and loop B of 20α-HSD. This product was ligated into the truncated pET-3α-HSD by using the internal *Eco*RI site and the second *Nco*I site. The 20α-HSD fragment containing loop-B extended from residues 169 to 232 and was larger than loop B alone. This fragment contained an additional six nonconservative

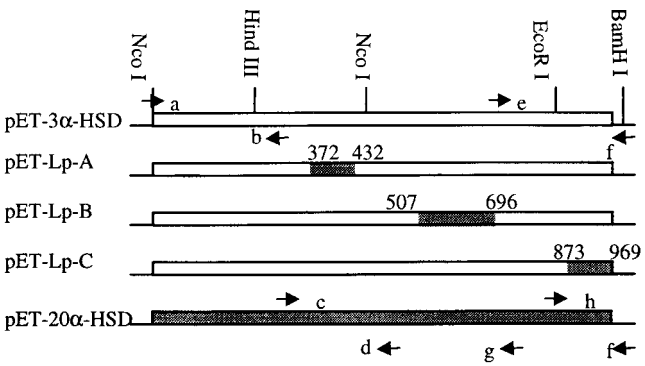

FIG. 2. Schematic of loop chimera construction. The arrows indicate the locations of oligonucleotide primers that were used for PCRs, and the small letters indicate the oligonucleotide sequences referenced in the text. The numbers indicate the nucleotide positions of the mutated loops. The positions of the swapped loops in the ternary complex also are shown in Fig. 1*b*.

mutations before loop B, which are unlikely to govern steroid specificity because of their positions within the structure (Fig. 1*b*).

The Lp-C chimera was generated by PCR amplification of the C terminus of 20α-HSD, which was ligated into the truncated pET-3α-HSD by using the *Eco*RI and *Bam*HI sites. The forward and reverse primers for amplification of the 20α-HSD loop C were 5′-dGCAGGTCTTTGAATTCCAGTTGGCTTC-3′ (h) and f, respectively. Multiple loop chimeras were constructed from the single chimeras.

Overexpression of Mutant and Chimeric Proteins. All proteins were overexpressed in $DH_{5\alpha}$ or C41 (DE3) *Escherichia coli* strains after the fidelity of their respective cDNAs was confirmed by dideoxysequencing. The latter strain was provided by J. E. Walker of the Medical Research Council Laboratory of Molecular Biology, Cambridge, U.K. All proteins were purified as described for recombinant 3α-HSD (17). Purification of recombinant 20α-HSD has been described (14).

Molecular Modeling. Molecular modeling was performed on a Indy Silicon Graphics workstation using the program QUANTA (Molecular Simulations, Waltham, MA). 3α-HSD·$NADP^+$·testosterone (1AFS, Protein Databank file) (1) was used as template. First, the apoprotein 20α-HSD structure was generated by mutating the amino acids of 3α-HSD to the appropriate residues in the target structure. Second, the ligands $NADP^+$ and testosterone were docked into the 20α-HSD model by using the coordinates of 3α-HSD·$NADP^+$·testosterone complex. Third, the 20α-HSD·$NADP^+$·progesterone complex was generated by removing testosterone and inserting progesterone so that its C20 ketone occupied the position of the C3 ketone of testosterone. In each case the models were locally energy-minimized by using the Adopted-Basis Newton Raphson algorithm with the program CHARMM (18).

Steady-State Kinetics and Product Identification. Specific activities for 3α- and 20α-HSDs were measured as follows: oxidation reactions contained either 75 μM androsterone or 40 μM 20α-OHP in 4% acetonitrile, 2.3 mM $NADP^+$, and 100 mM potassium phosphate buffer, pH 7.0; and reduction reactions contained either 35 μM 5α-DHT or 35 μM progesterone in 4% acetonitrile, 200 μM NADPH, and 100 mM potassium phosphate buffer, pH 6.0. Initial velocities were measured in a Beckman DU-640 spectrophotometer by observing the rate of change in absorbance of pyridine nucleotide at 340 nm (ε = 6,270 $M^{-1}\cdot cm^{-1}$). The limit of sensitivity of the assay is > μM/min per mg. Steady-state kinetic parameters were measured in the same assay using a range of androsterone or 20α-OHP concentrations while the cofactor concentration was kept constant (14, 17). 17β-HSD activity was monitored under similar conditions by using testosterone as substrate. The identity of steroid products was confirmed by radiochromatographic assays using [4-^{14}C] progesterone for 20α-HSD activity and [4-^{14}C] testosterone for 17β-HSD activity. Products were identified by cochromatography with authentic cold or radioactive steroids, which were visualized by spraying with a 1:1 methanol/H_2SO_4 solution or by autoradiography, respectively (14, 19).

RESULTS

Templates for Engineering HSDs in the AKR Superfamily. A common approach in protein engineering is to align the sequences of the starting and target structures. This approach is potentially powerful in HSDs in the AKR superfamily because they share greater than 67% amino acid sequence identity. Furthermore a crystal structure exists for the 3α-HSD·$NADP^+$·testosterone complex, which can be a structural model for other family members. This complex indicates that testosterone is bound in a pocket comprised of three large loops (an ordered loop A and the mobile loops B and C). Additional residues are recruited from two smaller loops that connect two β-strands and two α-helices (β_1-α_1 and β_2-α_2) in the $(\alpha/\beta)_8$ barrel motif (Fig. 1*b*). These five loops contribute 10 residues that form points of contact with testosterone. Alignment of these residues in HSDs within the AKR superfamily indicated that when 3α-HSD was compared with 20α-HSD six of 10 residues were different (Table 1). The conserved residues were either part of the catalytic tetrad Tyr-55 and His-117 or their nearest neighbors Leu-54 and Trp-118.

To predict which of the six residues confer specificity in 3α-HSD and 20α-HSD the steroid binding pockets of these two proteins were compared at the atomic level. A 20α-HSD·$NADP^+$·testosterone complex was built by using the coordinates for the 3α-HSD·$NADP^+$·testosterone complex. The 3α-HSD ternary complex depicts a perfect pocket for testosterone (Fig. 3*a*), but substitution of 20α-HSD residues resulted in significant clashes between the mutated residues and testosterone (Fig. 3*b*). Progesterone then was substituted in the 20α-HSD·$NADP^+$·testosterone complex to determine whether progesterone could fit the altered pocket. The resultant model predicted that altered residues could accommodate the binding of progesterone in a backwards orientation (D-ring at the A-ring position) and place the C17 side chain near the active site residues, which are essential changes if 20α-HSD activity is to be introduced. For example, when Asn-306 and Thr-24 were replaced by the bulkier Phe-306 and Tyr-24, the C17 side chain was channeled into position (Fig. 3*c*), whereas substitution of Thr-226 and Trp-227 with Tyr-226 and Cys-227 lead to the accommodation of the angular methyl groups in the A and D rings of progesterone (Fig. 3*d*).

Table 1. Alignment of steroid binding residues of HSDs in the AKR superfamily

	β1-α1*	β2-α2*		Loop A*			Loop B*		Loop C*	
HSD	Residue 24	Residue 54	Residue 55	Residue 117	Residue 118	Residue 129	Residue 226	Residue 227	Residue 306	Residue 310
Rat liver 3α-HSD (AKR1C9)†	T	**L**	**Y**	**H**	**F**	F	T	**W**	N	Y
Rat ovarian 20α-HSD (AKR1C8)	**Y**	**L**	**Y**	**H**	**F**	L	Y	C	F	M
Rabbit ovarian 20α-HSD (AKR1C5)	**Y**	M	**Y**	**H**	**F**	L	Q	**W**	I	S
Mouse liver 17β-HSD (AKR1C6)	**Y**	F	**Y**	**H**	**F**	L	E	**W**	V	F
Human type 1 3α-HSD (DD4) (AKR1C4)‡	**Y**	**L**	**Y**	**H**	**F**	L	L	**W**	V	F
Human type 2 3α-HSD (AKR1C3) (bifunctional 3α/17β-HSD)	**Y**	**L**	**Y**	**H**	S	S	R	**W**	F	S
Human type 3 3α-HSD (DD2) (AKR1C2)	**Y**	V	**Y**	**H**	**F**	I	P	**W**	L	I
Human 20α-HSD (DD1) (AKR1C1)	**Y**	**L**	**Y**	**H**	**F**	I	P	**W**	L	I

*The secondary structure motifs are defined by the ternary complex of 3α-HSD (1). Conserved residues are in bold.
†The nomenclature of the AKR superfamily is given in parenthesis (7).
‡Human isoforms are not positional and stereospecific steroid oxidoreductases; their names indicate the activities first assigned to these isoforms.

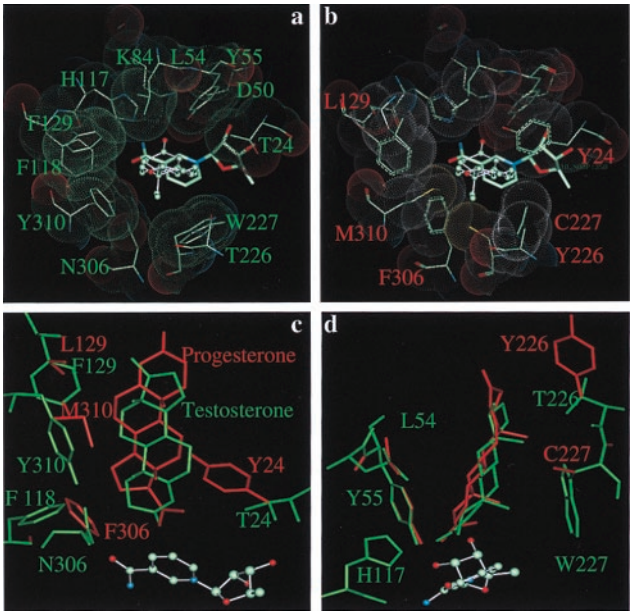

FIG. 3. Comparison of the substrate binding pockets of 3α- and 20α-HSDs. (*a*) The 3α-HSD testosterone binding pocket viewed from the top of the $(\alpha/\beta)_8$ barrel. (*b*) The 20α-HSD testosterone binding pocket viewed from the top of the $(\alpha/\beta)_8$ barrel to show the clashes with steroid ligand. (*c*) Side view to show the residues that directly interact with the edge of steroid hormones. (*d*) Side view to show the residues that directly interact with the α and β faces of steroid hormones. Testosterone and the binding pocket residues in 3α-HSD are labeled in green, and progesterone and the binding pocket residues in 20α-HSD are labeled in red.

Specific Activities of Point Mutants in the Substrate Binding Pocket. Based on the sequence alignment and modeling studies, individual and multiple amino acids in the pocket were mutated in an attempt to convert 3α-HSD to 20α-HSD. All mutants were expressed in *E. coli*, and SDS/PAGE was used to ensure that all mutants were similarly expressed (data not shown). Rather than purifying each of these mutants to homogeneity, the *E. coli* sonicates were assayed spectrophotometrically for 3α- and 20α-HSD activity (Table 2). The single mutants (T24Y, F129L) and the double mutant (N306F/Y310M) all retained activity (47–91 μM/min per mg) that was similar to a sonicate containing wild-type 3α-HSD (52 μM/min per mg). By contrast, the double mutant T226Y/W227C retained low 3α-HSD activity (2 μM/min per mg). Importantly, none of the mutants had 20α-HSD activity. Even when all the predicted mutations necessary to convert 3α-HSD into 20α-HSD were introduced, the resultant mutant T24Y/F129L/T226Y/W227C/N306F/Y310M had no 20α-HSD activity. Based on the sensitivity of our assay an inactive mutant has less than 0.01 μM/min per mg activity for 3α- or 20α-HSD substrates.

Table 2. Steroid specificity of 3α-HSD point mutants

	3α-HSD activity, μM/min per mg		20α-HSD activity, μM/min per mg	
Enzymes	Androsterone oxidation	5α-DHT reduction	20α-OHP oxidation	Progesterone reduction
3α-HSD	52	28	<0.01	<0.01
20α-HSD	<0.01	<0.01	158	173
T24Y	47	11	<0.01	<0.01
F129L	91	81	<0.01	<0.01
T226Y/W227C	2	5	<0.01	<0.01
N306F/Y310M	47	70	<0.01	<0.01

Enzymes containing the following point mutations: T24Y/T226Y/W227C; F129L/T226Y/W227C; T226Y/W227C/N306F/Y310M; F129L/T226Y/W227C/N306F/Y310M and T24Y/F129L/T226Y/W227C/N306F/Y310M had no detectable 3α-HSD or 20α-HSD activity (<0.01 μM/min per mg for androsterone and 20α-OHP oxidation). Activities were measured in *E. coli* sonicates.

Initial Characterization of Chimeric Proteins. Chimeric proteins then were constructed in which the steroid binding loops of 3α-HSD were replaced with loops of 20α-HSD. In designing these chimeras the two small loops, β_1-α_1 and β_2-α_2, were not replaced. Loop β_1-α_1 contributes only one residue to the binding pocket and with the exception of rat 3α-HSD is a Tyr in other 3α-, 17β-, and 20α-HSDs of the superfamily (Table 1). Loop β_2-α_2 was not swapped because it contains the catalytic residue Tyr-55. Other chimeric HSDs were overexpressed and purified to homogeneity from *E. coli* for kinetic characterization. The Lp-B chimera and double-loop chimeras Lp-AB and Lp-BC could not be kinetically characterized because their activity was too low. In each instance it is estimated that these chimeras oxidized less than 3 μM androsterone/min per mg as compared with 1.6 mM androsterone oxidized/min per mg by homogeneous recombinant 3α-HSD. These chimeras also displayed no 20α-HSD activity where the limit of detection would be 0.01 μM 20α-OHP oxidized/min per mg.

Steady-State Kinetic Properties of the Loop Chimeras. The kinetic properties of the active chimeric proteins, Lp-A, Lp-C, Lp-AC, and Lp-ABC, were compared by using $NADP^+$ as cofactor and androsterone, testosterone, or 20α-OHP as steroid substrates to measure the resultant 3α-, 17β-, and 20α-HSD activities, respectively (Table 3). In comparison with homogeneous recombinant 3α-HSD, the Lp-A chimera decreased the k_{cat} of androsterone oxidation 9-fold but increased K_m 60-fold, leading to an overall decrease in catalytic efficiency of 540-fold. The Lp-C chimera decreased the k_{cat} of androsterone oxidation only 5-fold but increased K_m 40-fold, which led to an overall decrease in catalytic efficiency of 200-fold. The Lp-A chimera introduced 17β-HSD activity and oxidized testosterone to androstenedione, with a k_{cat} of 1.8 min^{-1} and K_m of 1.8×10^{-4} M, which led to an overall catalytic efficiency of 1.0×10^4 $min^{-1} \cdot M^{-1}$. The shift in k_{cat}/K_m from 3α-HSD to 17β-HSD was 10^{10}, and the ratio of k_{cat}/K_m of 3α-HSD to 17β-HSD was 2:1. The Lp-AC chimera decreased the k_{cat} of androsterone 35-fold but only increased K_m 13-fold, which led to an overall decrease in catalytic efficiency of 460-fold. The Lp-AC chimera introduced 20α-HSD activity into the enzyme, which converted 20α-OHP to progesterone, with k_{cat} of 3.3 min^{-1} and K_m of 1.3×10^{-4} M, which led to an overall catalytic efficiency of 2.6×10^4 $min^{-1} \cdot M^{-1}$. The ratio of k_{cat}/K_m of 3α-HSD to 20α-HSD activity in this chimera was 1:1. Knowing that the Lp-B chimera abolished all 3α-HSD activity, Lp-B was introduced into the Lp-AC chimera. The Lp-ABC chimera was a positional and stereospecific 20α-HSD and oxidized 20α-OHP to progesterone, with k_{cat} of 2.4 min^{-1} and K_m of 1.2×10^{-4} M, which led to an overall catalytic efficiency of 2.1×10^4 $min^{-1} \cdot M^{-1}$. In this chimera, 3α-HSD was converted to a stereospecific 20α-HSD with a resultant shift in k_{cat}/K_m for the desired reaction of 2×10^{11} (Table 3, Fig. 4).

Identification of the Product of the 20α-HSD Reactions. To confirm that the loop chimeras produced the desired product of the 20α-HSD reaction, [^{14}C] progesterone was used as substrate with NADPH as cofactor (Fig. 5). The product was identified as 20α-OHP, and the results were consistent with the activities of the chimeras assigned by spectrophotometric assay. The Lp-AC and Lp-ABC chimeras had high 20α-HSD activity, and the chimeras Lp-AB and Lp-BC were inactive toward progesterone.

DISCUSSION

Maintenance of exquisite substrate specificity is a fundamental property of many enzymes. In particular, HSDs in the AKR superfamily use similar protein scaffolds to catalyze the positional and stereospecific oxidoreduction of steroids via the same mechanism. This divergent evolution is best demonstrated in rat liver

Table 3. Steady-state kinetic analysis of homogeneous recombinant 3α-HSD and 20α-HSD and the active loop chimeras

	3α-HSD	Lp-A	Lp-C	Lp-AC	Lp-ABC	20α-HSD
Androsterone					ND	ND
k_{cat} (min^{-1})	39.0 ± 1.2	4.5 ± 0.6	7.8 ± 0.6	1.2 ± 0.1		
K_m (M)	4.1×10^{-6}	2.5×10^{-4}	1.8×10^{-4}	5.5×10^{-4}		
k_{cat}/K_m ($min^{-1}\cdot M^{-1}$)	9.5×10^{6}	1.8×10^{4}	4.3×10^{4}	2.2×10^{4}		
Testosterone	ND		Insignificant	ND	ND	ND
k_{cat} (min^{-1})		1.8 ± 0.4				
K_m (M)		1.8×10^{-4}				
k_{cat}/K_m ($min^{-1}\cdot M^{-1}$)		1.0×10^{4}				
20α-OHP	ND	ND	ND			
k_{cat} (min^{-1})				3.3 ± 0.4	2.4 ± 0.4	63.7 ± 0.3
K_m (M)				1.3×10^{-4}	1.2×10^{-4}	7.5×10^{-6}
Lk_{cat}/K_m ($min^{-1}\cdot M^{-1}$)				2.6×10^{4}	2.1×10^{4}	8.5×10^{6}

ND, not detectable when 50–100 μg of purified protein was used. Insignificant, specific activity is <0.5 μM/min per mg for testosterone oxidation.

3α-HSD and rat ovarian 20α-HSD, which share 67% amino acid sequence identity, yet catalyze reactions on opposite ends of steroid hormone substrates.

Sequence Alignment and Molecular Modeling Studies Fail to Explain the Substrate Specificity of 3α- and 20α-HSD. Sequence alignment and molecular modeling studies using the 3α-HSD ternary complex as a template identified candidate residues that might be mutated to convert 3α-HSD to 20α-HSD. Because the C-terminal loop only becomes ordered upon binding steroid, it was predicted that the N306F/Y310M mutant would introduce 20α-HSD activity into 3α-HSD but this was not observed. Additionally the double mutant T226Y/W227C was predicted to accommodate the angular methyl groups of progesterone. However, this double mutant eliminated 3α-HSD activity but failed to introduce 20α-HSD activity into the protein. Modeling studies also predicted that a mutant containing Tyr-24, Tyr-226, Cys-227, and Phe-306 would meet all of the requirements to achieve productive progesterone binding, but surprisingly even when all the pocket residues in 3α-HSD were mutated to the corresponding residues in 20α-HSD (T24Y/F129L/T226Y/W227C/N306F/Y310M), this failed to convert 3α-HSD to 20α-HSD. These data suggest that sequence alignment and structural models are inadequate to explain the steroid hormone specificity of the two enzymes.

Single- or Double-Loop Chimeras Generated Bifunctional Enzymes. 3α- and 20α-HSD catalyze ordered bi-bi reactions in which NADP(H) must bind before steroid hormone substrate. Crystallographic studies on 3α-HSD indicate that the binding of ligand dictates loop movement. In the apoprotein 3α-HSD crystal structure only loop A is ordered (20), upon binding $NADP^+$ loop B becomes ordered (21), and when testosterone binds to form the 3α-HSD·$NADP^+$·testosterone ternary complex, the C-terminal loop (loop C) folds down onto the steroid (1). This observation led to the construction of the loop chimeras.

Steady-state kinetic studies indicated that the Lp-A chimera was a bifunctional 3α/17β-HSD and had a k_{cat} greater than the human type 2 3α-HSD (a bifunctional 3α/17β-HSD) (9). Testosterone is a competitive inhibitor of 3α-HSD and binds its C3-ketone in the active site in a position similar to a 3-ketosteroid substrate (Fig. 1*b*). However, for the enzyme to display 17β-HSD activity the pocket must have been altered so that it binds testosterone not only in the backwards orientation (D ring in the A ring position) but also upside down (β-face in the α-face orientation) to preserve the stereochemistry of hydride transfer. Thus the replacement of loop A of 3α-HSD with the corresponding loop in 20α-HSD to produce a flexible binding pocket, which can metabolize both 3α and 17β hydroxysteroids, was unexpected. Crystallographic studies of 3α-HSD indicated that loop A was the only ordered loop and its position was independent of the binding of cofactor or steroid (1, 20, 21). Our data indicate that loop A residues may be more plastic than originally proposed.

The Lp-B chimera eliminated all 3α-HSD activity but the Lp-C chimera maintained relatively high 3α-HSD activity. These results also were unexpected because loop C undergoes the most movement upon the binding of testosterone, and loop C has been implicated in substrate and inhibitor specificity in other AKRs (22, 23).

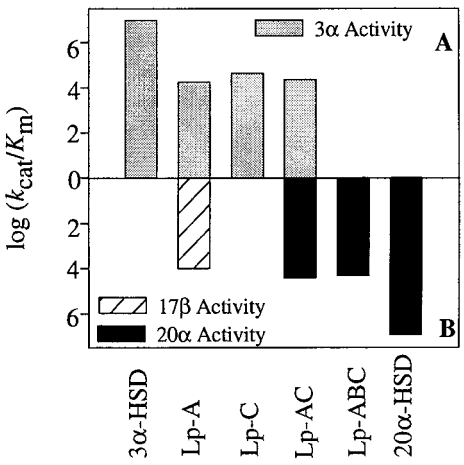

FIG. 4. Converting 3α-HSD into 20α-HSD by using chimeric constructs. The log k_{cat}/K_m values represented in Table 3 are plotted to demonstrate the progression from 3α- to 20α-HSD activity. (*A*) The log k_{cat}/K_m for 3α-HSD activity. (*B*) The log k_{cat}/K_m for 17β-HSD and 20α-HSD activity.

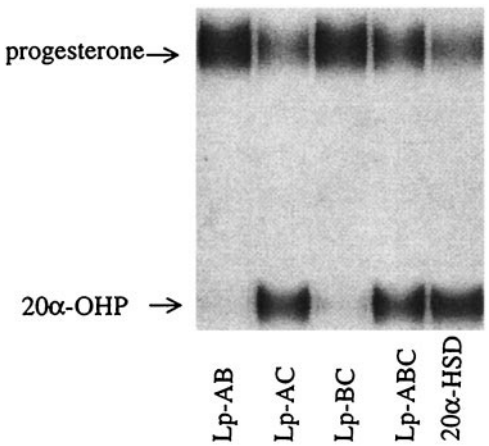

FIG. 5. 20α-OHP is identified as the product of [4-^{14}C] progesterone reduction catalyzed by the double- and triple-loop chimeras. Chimeras Lp-AC, Lp-ABC, and homogenous recombinant 20α-HSD all convert progesterone into 20α-OHP, but chimeras Lp-AB and Lp-BC failed to display this activity.

Double-loop chimeras Lp-AB and Lp-BC had such low 3α- and 20α-HSD activity that complete kinetic characterization was not possible. This finding also was surprising because Lp-BC contains both loops that undergo ligand-induced movement. Surprisingly, the Lp-AC chimera gave an enzyme that used both androsterone and 20α-OHP as substrates. This double-loop chimera thus had a new substrate-binding pocket that permits the backward binding of C21 steroids (D ring in the A ring position), but it did not allow the binding of steroids upside down (β-face in the α-face orientation). Thus the introduction of loop C of 20α-HSD made the pocket of the Lp-A chimera more discriminating.

Chimera Lp-ABC Created a 20α-HSD-Specific Enzyme. The Lp-ABC chimera that contained all three loops of 20α-HSD had no 3α-HSD activity but converted 3α-HSD into a positional and stereospecific 20α-HSD. This chimera displayed a k_{cat} comparable to the human 20α-HSD isoform (AKRICI), only its K_m was 10-fold higher (24). The catalytic efficiency of this chimera was still 404-fold less than homogeneous recombinant rat ovarian 20α-HSD, but a change in k_{cat}/K_m of 10^{11} was achieved for the desired reaction. This finding raises the issue as to why catalytic efficiency for wild-type 20α-HSD was not attained. Catalytic efficiency (k_{cat}/K_m) includes k_{cat} in the numerator, which in turn reflects the rate-limiting step. A combination of steady-state and transient kinetic studies (15, 25) and primary and solvent isotope effect measurements (26) indicate that the rate-limiting step in 3α-HSD is the chemical step that is governed by the catalytic tetrad (Tyr-55, His-117, Lys-84, and Asp-50) and its proximity to steroid substrate. These residues are in the core of the barrel in both enzymes and not on the loops that were replaced. By altering only the loops it is likely that the position of the substrate relative to the tetrad has been disturbed. Examination of the k_{cat} value for the Lp-ABC chimera indicates that it is reduced 27-fold and supports this concept. 3α- and 20α-HSD display ordered kinetic mechanisms (15, 27) in which k_{cat}/K_m reflects the chemical step and the binding and release of the second substrate. Therefore the remaining difference in catalytic efficiency is related to the binding and release of steroid, which may reflect that the engineered site has not been optimized for high-affinity steroid binding. The K_m value for the Lp-ABC chimera indicates that it is increased 15-fold.

Steroid-Induced Fit Plays a Dominant Role in Hormone Specificity in HSDs. Our approach demonstrates the limitations of two techniques used in protein engineering in a quest to alter substrate specificity. Site-directed mutagenesis dictated by computer models of steroid binding sites developed from crystallographic data has limited value unless structures exist for the ternary complexes of both the starting and target enzymes. Chimeric constructs gave the desired result with a higher degree of success. In our case, the conversion to the desired activity give a change in k_{cat}/K_m from a 3α-HSD to 20α-HSD of 2×10^{11}. In fact, few examples exist where the change has been so dramatic. In most cases, protein engineering has changed or broadened the preference of an enzyme for its intrinsic substrate selectivity (28–31), such as converting malate dehydrogenase to favor lactate (28) and converting trypsin to chymotrypsin to favor peptides with tryptophan, phenylanine, and tyrosine (29). In both of these examples the starting enzyme had residual activity for the target substrates.

To understand the structural basis of why the Lp-ABC chimera resembles 20α-HSD will require the determination of the crystal structures of both this chimera and native 20α-HSD preferably with $NADP^+$ and progesterone bound. The ability to introduce 20α-HSD activity via loop chimeras and not by point mutations of the steroid binding pocket suggests that the structural model was inadequate. The poor quality of this model may be explained if ligand induced-fit plays a dominant role in governing steroid specificity. This conclusion is supported by earlier studies in which point mutagenesis of tryptophans on opposite side of the steroid pocket of 3α-HSD revealed that diverse ligands bind to the same pocket differently (32). Our studies suggest that upon the binding of substrate loops A, B, and C may move and that the residues recruited from the loops to form the mature pocket will depend on the protein structure and will be dictated by ligand. Thus the residues that comprise a mature binding pocket are unlikely to be predicted by merely aligning residues on loop structures dictated by a single ternary complex structure.

We thank Drs. K. Ratnam and J.M. Jez for their valuable advice. This work was supported by National Institutes of Health Grant DK47015 to T.M.P., and H.M. was partially supported by a National Institutes of Health Predoctoral Training Grant in Pharmacology.

1. Bennett, M. J., Albert, R. H., Jez, J. M., Ma, H., Penning, T. M. & Lewis, M. (1997) *Structure (London)* **5,** 799–812.
2. Breton, R., Housset, D., Mazza, C. & Fontecilla-Camps, J. C. (1996) *Structure (London)* **4,** 905–915.
3. Williams, S. P. & Sigler, P. B. (1998) *Nature (London)* **393,** 392–396.
4. Brzozowski, A. M., Pike, A. C., Dauter, Z., Hubbard, R. E., Bonn, T., Engstrom, O., Ohman, L., Greene, G. L., Gustafsson, J. A. & Carlquist, M. (1997) *Nature (London)* **389,** 753–758.
5. Penning, T. M. (1997) *Endocr. Rev.* **18,** 281–305.
6. Jez, J. M., Bennett, M. J., Schlegel, B. P., Lewis, M. & Penning, T. M. (1997) *Biochem. J.* **326,** 625–636.
7. Jez, J. M., Flynn, T. G. & Penning, T. M. (1997) *Biochem. Pharmacol.* **54,** 639–647.
8. Taurog, J. D., Moore, R. J. & Wilson, J. D. (1975) *Biochemistry* **14,** 810–817.
9. Lin, H. K., Jez, J. M., Schlegel, B. P., Peehl, D. M., Pachter, J. A. & Penning, T. M. (1997) *Mol. Endocr.* **11,** 1971–1984.
10. Dufort, I., Soucy, P., Labrie, F. & Luu-The, V. (1996) *Biochem. Biophys. Res. Commun.* **228,** 474–479.
11. Wiest, W. G., Kidwell, W. R. & Balogh, K., Jr. (1968) *Endocrinology* **82,** 844–859.
12. Lenton, E. A. & Woodward, A. J. (1988) *J. Reprod. Fertil.* **36,** Suppl., 1–15.
13. Talalay, P. & Levy H. R. (1959) in *Steric Course of Microbiological Reactions*, eds. Wolstenholme, G. E. W. & O'Connor, C. M. (Little Brown, Boston), pp. 53–78.
14. Ma, H. & Penning T. M. (1999) *Biochem. J.* **341,** 853–859.
15. Askonas, L. J. Ricigliano, J. W. & Penning, T. M. (1991) *Biochem. J.* **278,** 835–841.
16. Kersey, W. H. & Wilcox R. B. (1970) *Biochemistry* **9,** 1284–1286.
17. Pawlowski, J. E. & Penning, T. M. (1994) *J. Biol. Chem.* **269,** 13502–13510.
18. Buczko, E., Koh, Y. C., Miyagawa, Y. & Dufau, M. L. (1994) *J. Steroid Biochem. Mol. Biol.* **52** 209–218.
19. Jez, J. M. & Penning, T. M. (1998) *Biochemistry* **37,** 9695–9703.
20. Hoog, S. S., Pawlowski, J. E., Alzari, P. M., Penning, T. M. & Lewis, M. (1994) *Porc. Natl. Acad. Sci. USA* **91,** 2517–2521.
21. Bennett, M. J., Schlegel, B. P., Jez, J. M., Penning, T. M. & Lewis, M. (1996) *Biochemistry* **35,** 10702–10711.
22. Bohren, K. M., Grimshaw, C. E. & Gabbay, K. H. (1992) *J. Biol. Chem.* **267,** 20965–20970.
23. Barski, O. A., Gabbay, K. H. & Bohren, K. M. (1996) *Biochemistry* **35,** 14276–14280.
24. Hara, A., Matsuura, K., Tamada, Y., Sato, K., Miyabe, Y., Deyashiki, Y. & Ishida, N. (1996) *Biochem. J.* **313,** 373–376.
25. Ratnam, K., Ma, H. & Penning, T. M. (1999) *Biochemistry* **38,** 7856–7864.
26. Ratnam, K., Ma, H. & Penning, T. M. (1999) *FASEB. J.* **13,** A1113 (abstr.).
27. Pongsawasdi, P. & Anderson, B. M. (1984) *Biochim. Biophys. Acta* **799,** 51–58.
28. Wilks, H. M., Hart, K. W., Feeney, R., Dunn, C. R., Muirhead, H., Chia W. N., Barstow, D. A., Atkinson, T., Clarke, A. R. & Holbrook, J. J. (1988) *Science* **242,** 1541–1544.
29. Hedstrom, L., Szilagyi, L. & Rutter, W. J. (1992) *Science* **255,** 1249–1253.
30. Curnow, K. M., Mulatero, P., Emeric-Blanchouin, N., Aupetit-Faisant, B., Corvol, P. & Pascoe, L. (1997) *Nat. Struct. Biol.* **4,** 32–35.
31. Bone, R., Silen, J. L. & Agard, D. A. (1989) *Nature (London)* **339,** 191–195.
32. Jez, J. M., Schlegel, B. P. & Penning, T. M. (1996) *J. Biol. Chem.* **271,** 30190–30198.